Journal of Physiology (1993), **470**, *pp.* 109–126
With 8 figures
Printed in Great Britain

THE EFFECTS OF LOW CALCIUM ON THE VOLTAGE-DEPENDENT CONDUCTANCES INVOLVED IN TUNING OF TURTLE HAIR CELLS

BY J. J. ART*, R. FETTIPLACE† AND Y.-C. WU

*From the Department of Neurophysiology, University of Wisconsin Medical School, Madison, WI 53706, and the *Department of Pharmacological and Physiological Sciences, University of Chicago, Chicago IL 60637, USA*

(*Received 9 November 1992*)

SUMMARY

1. The voltage-dependent conductances of turtle cochlear hair cells of known resonant frequency were characterized by tight-seal, whole-cell recording during superfusion with solutions containing normal (2·8 mM) and reduced (0·1–10 μM) Ca^{2+}.

2. In 1 μM Ca^{2+}, the current flowing through the voltage-dependent Ca^{2+} channels was increased roughly fivefold and had a reversal potential near 0 mV. This observation may be explained by the Ca^{2+} channels becoming non-selectively permeable to monovalent cations in low-Ca^{2+} solutions. Lowering the Ca^{2+} further to 0·1 μM produced little increase in the current.

3. The size of the non-selective current increased systematically with the resonant frequency of the hair cell over the range from 10 to 320 Hz. This suggests that hair cells tuned to higher frequencies contain more voltage-dependent Ca^{2+} channels.

4. There was a good correlation between the amplitudes of the non-selective current and the K^+ current which underlies electrical tuning of these hair cells. The amplitude of the K^+ current also increased systematically with resonant frequency.

5. In cells with resonant frequencies between 120 and 320 Hz, the K^+ current was completely abolished in 1 μM Ca^{2+}, consistent with prior evidence that this current flows through Ca^{2+} activated K^+ channels. In a majority of cells tuned between 50 and 120 Hz, the K^+ current was incompletely blocked in 1 μM Ca^{2+}, but was eliminated in 0·1 μM Ca^{2+}. In all hair cells the K^+ current was abolished by 25 mM tetraethylammonium chloride.

6. In cells tuned to 10–20 Hz, the K^+ current was not substantially diminished even in 0·1 μM Ca^{2+}, which argues that it may not be Ca^{2+} activated.

7. In cells tuned to frequencies above 100 Hz, the K^+ current could still be evoked by depolarization during superfusion with 10 μM Ca^{2+}. However, its half-activation voltage was shifted to more depolarized levels and its maximum amplitude was systematically reduced with increasing resonant frequency.

8. These observations are consistent with the notion that in cells tuned to more than 50 Hz, there is a fixed ratio of the number of voltage-dependent Ca^{2+} channels

† To whom reprint requests should be addressed.

MS 1889

to Ca^{2+}-activated K^+ channels, the numbers of each increasing in proportion to resonant frequency. The results also provide indirect evidence that the Ca^{2+}-activated K^+ channels in cells tuned to higher frequencies may be less sensitive to intracellular Ca^{2+}.

INTRODUCTION

Both auditory and vestibular hair cells of many lower vertebrates have a membrane impedance resembling a simple resonator which causes them to be tuned to a specific frequency in the mechanical stimulus (for review see Fettiplace, 1987). Such tuning is thought to arise from the interaction of a voltage-dependent Ca^{2+} current and a Ca^{2+}-activated K^+ current (Lewis & Hudspeth, 1983; Art & Fettiplace, 1987; Hudspeth & Lewis, 1988; Fuchs, Nagai & Evans, 1988). In the turtle's basilar papilla, hair cells possess resonant frequencies from 10 Hz to over 500 Hz (Crawford & Fettiplace, 1981), this range being achieved by changes in the number of K^+ channels per cell and in the kinetics of the K^+ current, which has a time constant varying from about 150 ms in low-frequency cells to less than 1 ms in high-frequency cells (Art & Fettiplace, 1987). An important remaining question concerns the mechanism by which the kinetics of the K^+ current are varied.

One potential variable controlling the properties of the K^+ current could be the intracellular Ca^{2+} concentration, since previous work (Art & Fettiplace, 1987) suggested that there may also be a systematic variation in the number of Ca^{2+} channels per hair cell. The relative sizes of the Ca^{2+} and K^+ currents in a given cell were compared by quantifying the K^+ current and then blocking it either with tetraethylammonium ions (TEA) or with Ba^{2+}. The two methods gave conflicting results, though both treatments were imperfect and caused some cellular deterioration. Similar problems were reported in the chick cochlea by Fuchs, Evans & Murrow (1990) who found no correlation in the size of the Ca^{2+} current with the location of the hair cell, but a threefold difference in Ba^{2+} currents between populations of cells tuned to low and high frequencies. Thus one aim of the present work was to devise another technique for characterizing both K^+ and Ca^{2+} currents in hair cells of known resonant frequency. We employed the observation that when the extracellular Ca^{2+} concentration is very low, current through the Ca^{2+} channels is carried mainly by monovalent cations (Almers & McCleskey, 1984; Hess & Tsien, 1984); in such conditions, the Ca^{2+} influx should be insufficient to activate the K^+ current. Our results demonstrate a clear correlation between the size of the Ca^{2+} current and the K^+ current.

METHODS

Preparation and recording techniques

Methods for isolation and electrical recording from single hair cells were identical to those described previously (Art & Fettiplace, 1987). Briefly, turtles (*Pseudemys scripta elegans*, carapace length about 12 cm), were decapitated, the basilar papilla dissected out and hair cells isolated following incubation in a saline containing 0·1 mM Ca^{2+} to which had been added 0·5 mg papain ml^{-1}, 5 mg bovine serum albumin ml^{-1}, 2·5 mM L-cysteine and 10 μg DNAase ml^{-1}. Cells were plated onto a clear glass coverslip and transferred for experiments to the stage of a Zeiss IM-35 inverted microscope. Membrane currents were measured using the whole-cell patch clamp technique with a List EPC-7 amplifier. Soda-glass recording pipettes (resistances 2–3 MΩ) were usually filled with a solution containing (mM): KCl, 125; $MgCl_2$, 3; K_2EGTA, 5; Na_2ATP, 2·5; KHepes, 5; pH 7·2. For experiments to measure directly the voltage-dependent Ca^{2+} current, the

patch electrode was filled with a Cs^+-based solution of composition (in mM): CsCl, 125; $MgCl_2$, 3; Na_2EGTA, 5; Na_2ATP, 2·5; NaHepes, 5; pH 7·2. The time constant of the recording system, estimated from the product of the cell capacitance and the uncompensated series resistance, was 20–60 μs. The capacitance of most cells was in the range 7–12 pF. Membrane currents were recorded on a Sony PC108M Instrumentation Recorder at a bandwidth of 20 kHz, and on playback were low-pass filtered (8-pole Bessel) with 3 dB at either 2 or 15 kHz for digitization at 6 or 50 kHz respectively. Between two and twenty current responses were usually averaged for each experimental condition and corrected for any ohmic leakage conductance determined from 5 mV depolarizing voltage steps from −84 mV. In constructing current–voltage relationships, all steady-state membrane potentials were corrected for the measured junction potential and for incomplete compensation of the electrode's series resistance. Experiments were performed at 22–24 °C.

Solutions

Experiments were begun in a control solution containing (mM): NaCl, 130; KCl, 4; $MgCl_2$, 2·2; $CaCl_2$, 2·8; glucose, 8; NaHepes, 5; pH 7·6. The ionic environment of a cell was rapidly changed using either a U-tube system (Krishtal & Pidoplichko, 1980) or a three-barrelled glass 'pan-pipe' (Yellen, 1982). Each barrel of the pan-pipe was of square cross-section pulled to an internal diameter of about 50 μm and perfused from a peristaltic pump, a given barrel being selected by means of a remotely controlled miniature solenoid valve (Lee Products, Westbrook, CT, USA). With the latter method the solution bathing a cell could be exchanged in less than 100 ms. In the test solutions, the Mg^{2+} was removed and the Ca^{2+} was buffered at low concentrations with either 5 mM BAPTA (0·1 μM Ca^{2+}) or 5 mM HEDTA (1 and 10 μM Ca^{2+}). The proportions of buffer and total Ca^{2+} needed to achieve a given free Ca^{2+} were calculated (Fabiato & Fabiato, 1979; Schoenmakers, Visser, Flik & Theuvenet, 1992) and the free Ca^{2+} concentration was measured with a Ca^{2+}-sensitive electrode (Tsien & Rink, 1981) and found to be no more than 20% different from the expected value.

RESULTS

The effects of 1 μM Ca^{2+}

Turtle hair cells contain two major voltage-dependent currents, a Ca^{2+} current and a much larger Ca^{2+}-activated K^+ current. Figure 1*A* illustrates the most common effect of lowering the external Ca^{2+} to 1 μM, where the outward net current to a depolarizing voltage step was replaced by an inward current. Steady-state current–voltage relationships in normal and 1 μM Ca^{2+} are shown for this cell in Fig. 2*A*. In previous experiments on hair cells, inward currents in low-Ca^{2+} solutions had been attributed to activation of the mechano-electrical transducer conductance (Crawford, Evans & Fettiplace, 1991), but this cannot be the explanation for the present results since: (i) the inward current was reversibly abolished by the Ca^{2+} channel antagonist nifedipine at 20 μM (Fig. 2*A*); (ii) the steady-state current–voltage relationship had the U-shaped form of the voltage-dependent Ca^{2+} current, but with a reversal potential near 0 mV (mean = −2 mV, $n = 7$); (iii) the transducer conductance is known to be irreversibly blocked by brief exposures to 1 μM Ca^{2+} (Crawford *et al.* 1991). The simplest explanation for the results is that the current is flowing through voltage-dependent Ca^{2+} channels, but when the external Ca^{2+} concentration is very low, these channels become non-selectively permeable to monovalent cations (Almers & McCleskey, 1984; Hess & Tsien, 1984).

Lowering extracellular Ca^{2+} to 1 μM caused complete block of the outward K^+ current in all cells tuned to frequencies higher than 120 Hz, but more complicated effects were observed in lower frequency cells. These anomalies may be divided into two categories according to resonant frequency: those tuned between 50 and 120 Hz, and those tuned to 10–20 Hz (no recordings were obtained from cells with resonant frequencies between 20 and 50 Hz). Four out of seven cells in the former category

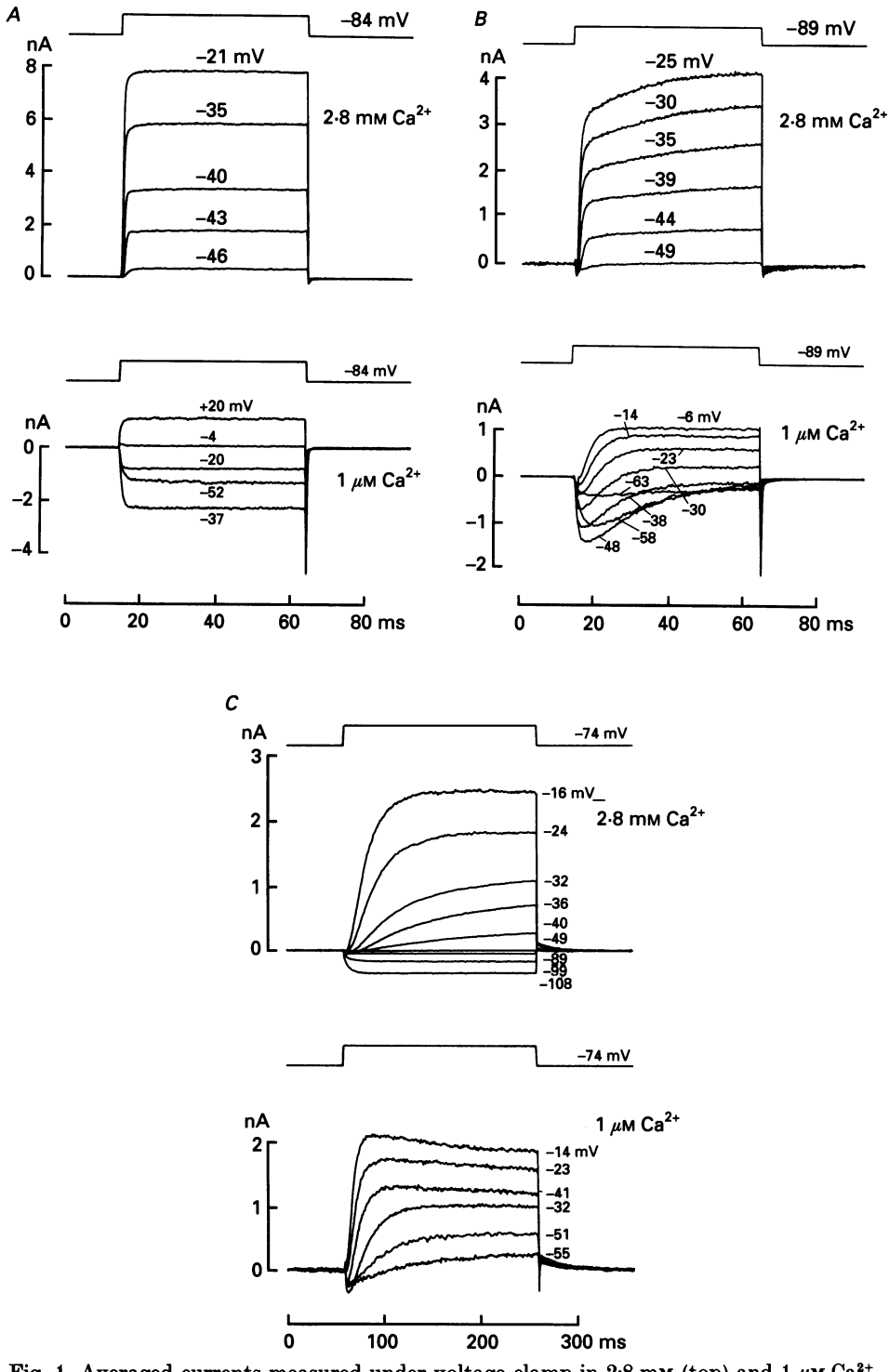

Fig. 1. Averaged currents measured under voltage clamp in 2·8 mM (top) and 1 μM Ca^{2+} (bottom) for three different hair cells of resonant frequency 253 Hz (*A*), 118 Hz (*B*) and 10 Hz (*C*). Membrane potentials during the step are indicated next to the traces and the

exhibited biphasic responses in 1 μM Ca^{2+} (Fig. 1*B*) and had a significant outward current near 0 mV, where the non-specific current should have been small. This outward current had a reversal potential around −80 mV, near the K^+ equilibrium potential, and it was turned on at membrane potentials positive to −50 mV, so its activation presumably accounts for the sag in the non-specific inward current. For three cells tuned between 10 and 20 Hz, the amplitude of the K^+ current was only slightly diminished in 1 μM Ca^{2+} (Fig. 1*C*).

Despite the complex effects of 1 μM Ca^{2+} on the outward K^+ currents according to the resonant frequency of the hair cell, all cells showed evidence of a non-specific inward current in low Ca^{2+}. The current at the onset of small voltage-clamp steps was inward going, and there was a fast inward tail current on repolarization to membrane potentials near the K^+ equilibrium potential (Fig. 1).

Quantitative relationship between Ca^{2+} and non-specific currents

In order to study the relationship between the non-specific current and the voltage-dependent Ca^{2+} current without interference from the K^+ current, measurements were made with Cs^+-filled electrodes (Fig. 3). The non-specific current in 1 μM Ca^{2+} is slightly slower but about five times larger than the corresponding Ca^{2+} current. The activation of the two conductances was inferred from measurements of the amplitudes of the tail currents, and the results (Fig. 3*C*) were fitted with a Boltzmann function

$$I = I_{max}/[1+\exp((V_0-V)/V_e)], \quad (1)$$

enabling the maximum current, I_{max}, the voltage sensitivity (V_e) and half-activation voltage (V_0) to be determined. Both currents were activated e-fold in about 8 mV, but the half-activation for the non-selective current was shifted to more negative membrane potentials. In four cells the ratio of the maximum currents in reduced and normal Ca^{2+} was 4·5 ± 0·1 (mean ± S.D.) and the hyperpolarizing shift was 20 ± 3 mV. About 90% of the non-specific current could be reversibly blocked by 20 μM nifedipine. Although nifedipine at these concentrations is known also to block voltage-dependent K^+ currents (Nerbonne & Gurney, 1987), this cannot be its mode of action here since the K^+ currents were already abolished by the presence of intracellular Cs^+.

The non-specific current was only slightly augmented by lowering the extracellular Ca^{2+} concentration from 1 to 0·1 μM Ca^{2+}, but its amplitude was reduced to about one-fifth in 10 μM Ca^{2+}. In two experiments (not shown), plots of the amplitude of the non-specific current as a function of extracellular Ca^{2+} concentration gave values of about 3 μM for the dose of Ca^{2+} required to half-block the non-specific current, which is comparable to that found in other preparations (0·7 μM, Almers, McCleskey & Palade, 1984; 2 μM, Lux, Carbone & Zucker, 1989). The shift of the activation curve to more negative membrane potentials was similar in all Ca^{2+} concentrations below 10 μM. For example, in one experiment, the observed shifts were 20, 20 and 24 mV

holding potentials were −84 mV (*A*), −89 mV (*B*) and −74 mV (*C*). Note that the low Ca^{2+} completely eliminates the outward current at negative membrane potentials in *A*, the cell tuned to the highest frequency, but not in the lower frequency cells, *B* and *C*. However, in all three cells, fast inward tail currents are evident at the end of the voltage step.

in 10, 1 and 0·1 μM Ca^{2+} respectively. This hyperpolarizing shift may reflect a surface-charge effect (Frankenhaeuser & Hodgkin, 1956), whereby negative charges on the external surface of the membrane are unmasked by removal of Ca^{2+} (and Mg^{2+}), hence reducing the field within the membrane.

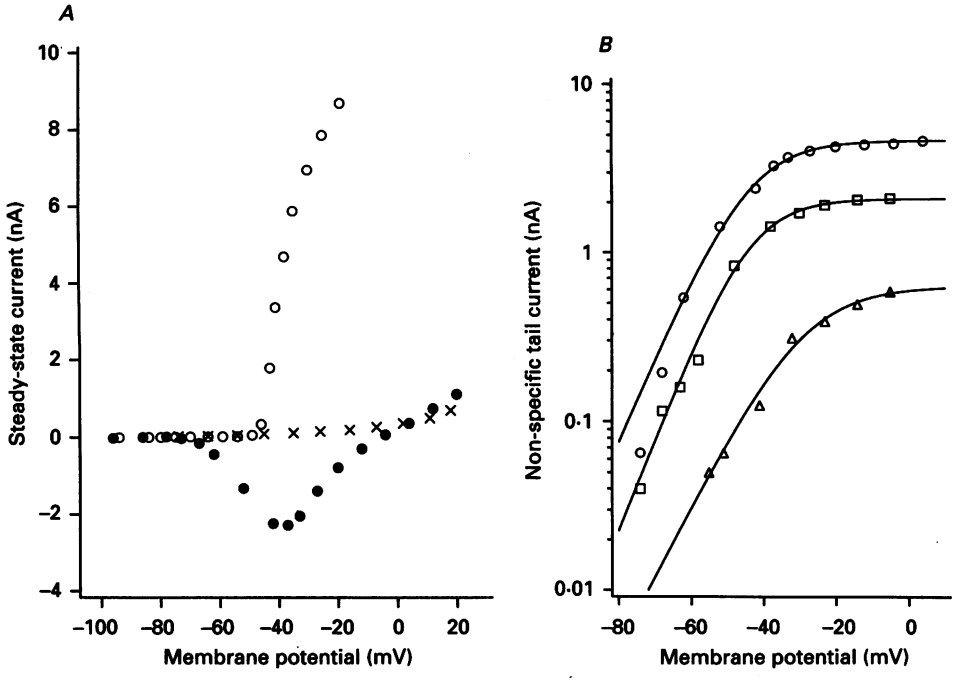

Fig. 2. *A*, steady-state current–voltage relationships for the cell in Fig. 1*A* in 2·8 mM (○) and 1 μM Ca^{2+} (●). The inward current in 1 μM Ca^{2+} was abolished by 20 μM nifedipine (×). *B*, plots of the tail current in 1 μM Ca^{2+} against membrane potential for the three hair cells of different resonant frequency whose records are shown in Fig. 1. All membrane potentials corrected for the electrode's residual series resistance. Each set of points was fitted by eqn (1). Note that the saturated current increases with resonant frequency. Resonant frequency, membrane capacitance and fitting parameters (I_{max}, V_0 and V_e): ○, 253 Hz, 9 pF, 4·6 nA, −44 mV, 8·8 mV; □, 118 Hz, 8 pF, 2·1 nA, −44 mV, 8·0 mV; △, 10 Hz, 7·4 pF, 0·62 nA, −30 mV, 10·4 mV.

Correlation of the size of the non-specific current with resonant frequency

The aim of subsequent experiments was to employ the non-specific current as a measure of the voltage-dependent Ca^{2+} current. Experiments were performed with K^+-filled electrodes to allow simultaneous characterization of the K^+ current and measurement of the hair cell's resonant frequency from the frequency of the oscillations in membrane potential to small current pulses (Crawford & Fettiplace, 1981). The amplitude of the non-specific current could be inferred from the inward tail currents, which are plotted against membrane potential in Fig. 2*B* for the three cells illustrated in Fig. 1. The tail currents activate over a similar range in all three cells but the maximum current is about eight times larger in the cell tuned to the highest frequency (253 Hz) than in the cell tuned to the lowest frequency (10 Hz).

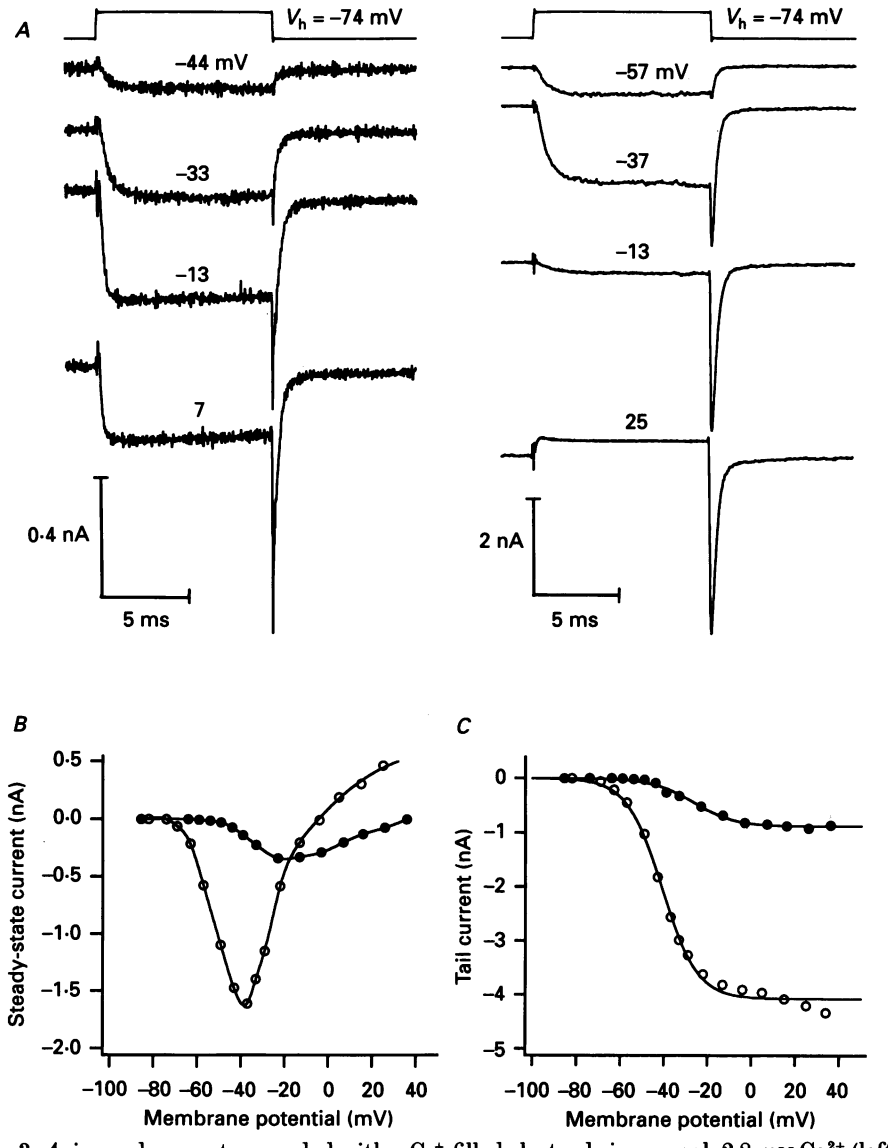

Fig. 3. *A*, inward currents recorded with a Cs^+-filled electrode in normal, 2·8 mM Ca^{2+} (left) and 1 μM Ca^{2+} (right). The responses in normal Ca^{2+} represent the voltage-dependent Ca^{2+} current. Traces are averages of two responses (left) and five responses (right). *B*, steady-state current–voltage relationships derived from currents in *A*. *C*, measurements of the tail currents in normal (●) and 1 μM Ca^{2+} (○). The points have been fitted with eqn (1) with parameters (I_{max}, V_o and V_e): 2·8 mM Ca^{2+}, 0·88 nA, −26 mV, 8·6 mV; 1 μM Ca^{2+}, 4·1 nA, −41 mV, 8·1 mV. In low Ca^{2+} the maximum current increased 4·6-fold, and the half-activation shifted 15 mV in the hyperpolarizing direction.

Collected results of the maximum amplitude of the non-specific tail current for twelve cells displaying sharp tuning, which enabled accurate estimates of their resonant frequencies, are given in Fig. 4*A*. These results demonstrate a clear

correlation between the size of the non-specific current and resonant frequency and, on the assumption that the size of the single Ca^{2+} channel is similar in all cells, indicate that higher frequency cells have a larger number of voltage-dependent Ca^{2+} channels. As shown in Fig. 1, 1 μM Ca^{2+} did not completely eliminate the outward K^+

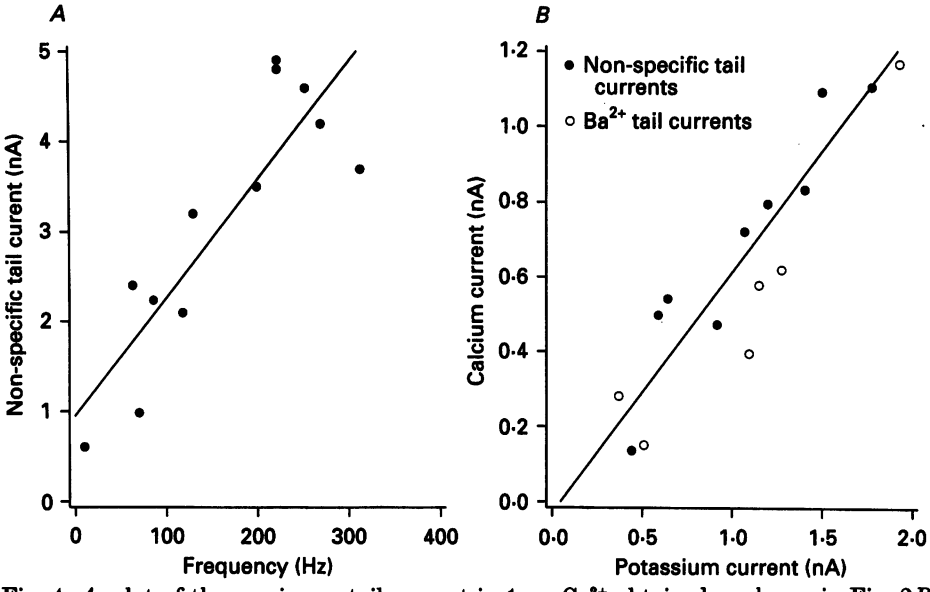

Fig. 4. *A*, plot of the maximum tail current in 1 μM Ca^{2+} obtained as shown in Fig. 2*B* against the resonant frequency of the hair cell for twelve cells. Since the holding potential was slightly different in different experiments, the values were corrected to a holding potential of −84 mV, assuming a reversal potential of 0 mV. Line drawn through points is least-squares fit, $r = 0{\cdot}92$. *B*, plot of the maximum Ca^{2+} current against the maximum K^+ current in fifteen cells. Filled symbols were from experiments illustrated in *A*, the Ca^{2+} current being obtained by dividing the non-specific tail current by 4·5. Open symbols were from previous experiments (Art & Fettiplace, 1987), where Ba^{2+} was used to block the K^+ current and Ca^{2+} currents inferred using a measured Ba^{2+}:Ca^{2+} conductance ratio of 3:1. In all experiments, the saturated K^+ current was obtained from tail current measurements in normal saline from a holding potential of about −50 mV. Line is least-squares fit; $r = 0{\cdot}97$, slope = 0·64.

current in cells tuned to less than 120 Hz. However, this did not impair quantification of the non-selective tail current since measurements were taken near the K^+ equilibrium potential and also the non-specific tail current was fast compared to any residual outward current. Variations in the amplitude of the non-specific current could not be accounted for by differences in cell size. Although there were variations in membrane capacitance from 7·4 to 11 pF in the cells plotted, there was no overall trend with resonant frequency (Art & Fettiplace, 1987). No attempt was made to normalize the current to the cell capacitance, since the Ca^{2+} channels are likely to be absent from the hair cell's apical pole which makes a significant and possibly variable contribution to the cell's membrane area.

Figure 4*B* shows the correlation between the sizes of the Ca^{2+} and K^+ currents for those cells in which a complete set of data was available. Plotted on the ordinate is

the size of the Ca^{2+} current, derived by dividing the non-specific tail current by the factor of 4·5 inferred from the measurements above. On the abscissa is plotted the amplitude of the K^+ current, which was obtained by measuring the saturating tail current in normal extracellular Ca^{2+} at a holding potential of about −48 mV (see Fig.

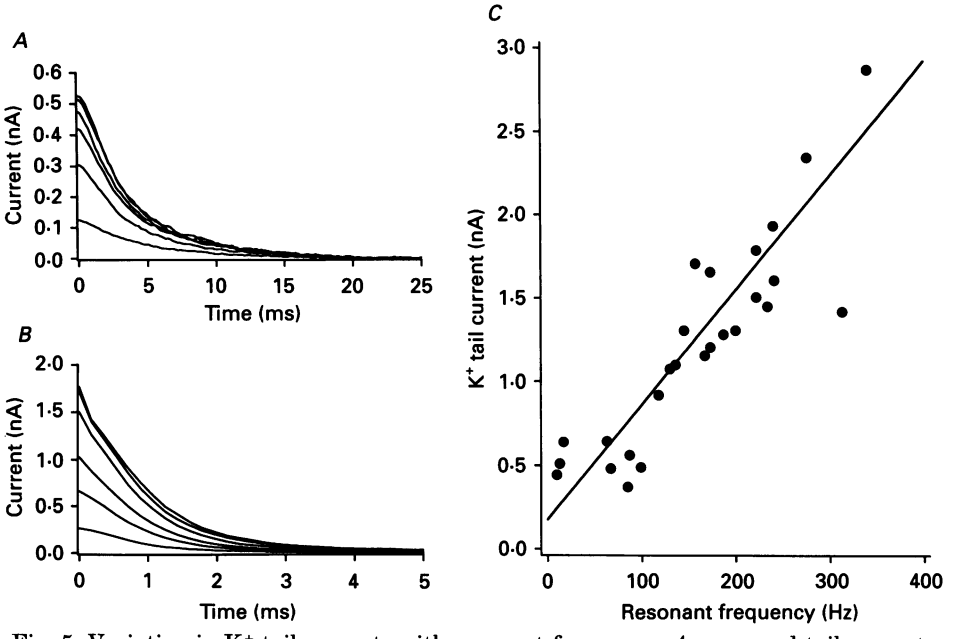

Fig. 5. Variation in K^+ tail currents with resonant frequency. *A*, averaged tail currents, for cell tuned to 87 Hz, evoked at the termination of voltage steps to −17, −25, −33, −36, −40 and −44 mV returning to a holding potential of −48 mV. *B*, averaged tail currents, for cell tuned to 222 Hz, at the end of voltage steps to −25, −31, −36, −37·5, −39 and −41 mV, holding potential −49 mV. Note the differences in axis scaling, the tail currents being both larger and faster in the higher frequency cell. The time constant of decay of the current for the smallest voltage steps was 4·8 ms (*A*) and 0·94 ms (*B*). *C*, plot of the saturating amplitude of the K^+ tail current *versus* resonant frequency for twenty-six cells. Straight line is least-squares fit: $r = 0{\cdot}88$.

5*A* and *B*). Since the K^+ current is slower and larger than the Ca^{2+} current, this method should provide an accurate estimate of its amplitude uncontaminated by the Ca^{2+} current. Also included in Fig. 4*B* are values obtained from experiments in which Ba^{2+} was used to block the K^+ current, and the Ba^{2+} currents have been scaled by 0·33 to take account of the differences in permeability to Ca^{2+} and Ba^{2+} (Art & Fettiplace, 1987). The plot displays an excellent correlation between the two parameters for cells tuned over the frequency range from 10 to 313 Hz. One conclusion from these measurements is that the hair cells maintain a constant ratio of numbers of Ca^{2+} to K^+ channels, and that both numbers increase in proportion to the cell's resonant frequency.

The method for determining the size of the K^+ current is shown in Fig. 5. The amplitude of the tail current, evoked on repolarization to about −48 mV (near the resting potential of the cell), increased and eventually saturated for large depolarizing

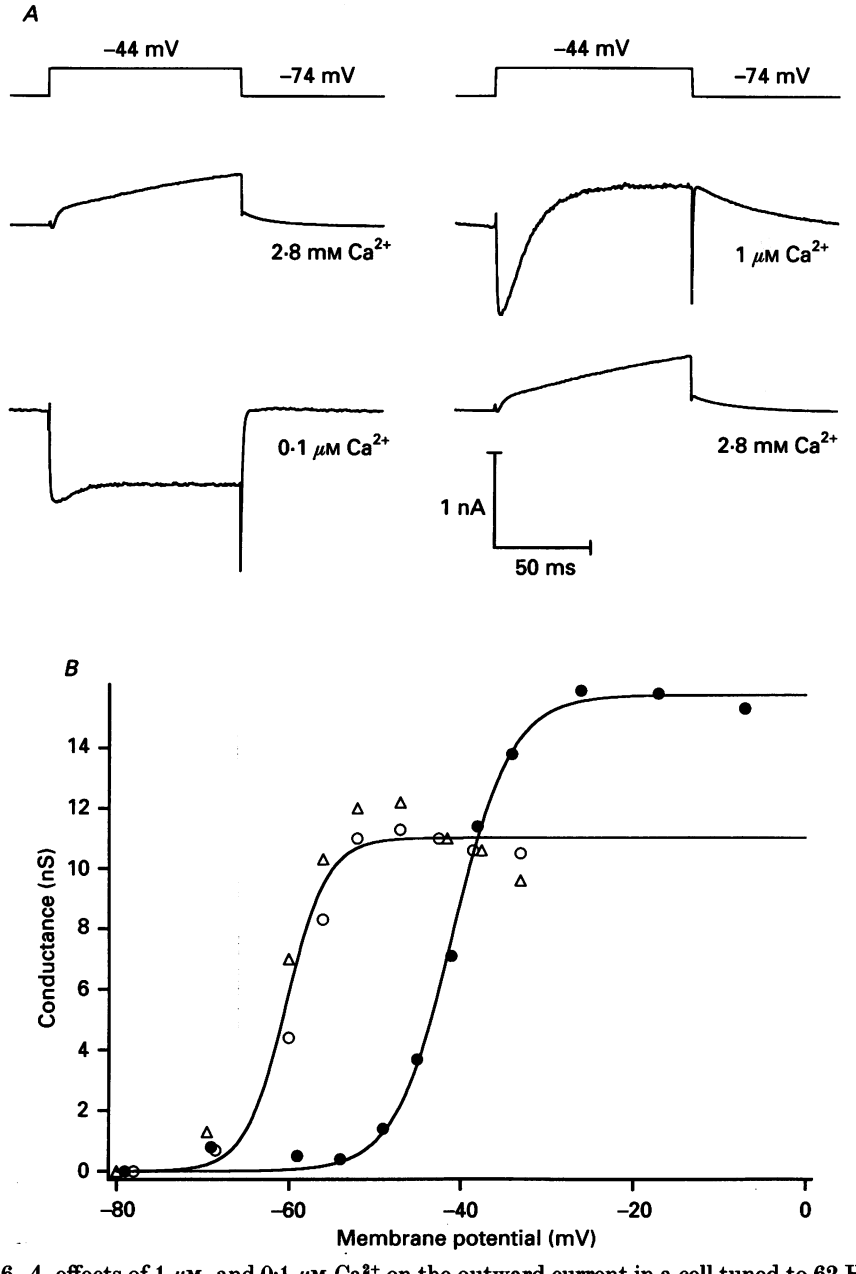

Fig. 6. *A*, effects of 1 μM- and 0·1 μM-Ca^{2+} on the outward current in a cell tuned to 62 Hz. Lowering the Ca^{2+} to 1 μM produced a biphasic current as in Fig. 1*B*, but most of the outward current could be eliminated by reducing the Ca^{2+} further to 0·1 μM. *B*, activation curves for the K^+ conductance in a very low-frequency hair cell in normal Ca^{2+} (●), in 1 μM-Ca^{2+} (○) and 0·1 μM-Ca^{2+} (△). Since the measurements in the two low-Ca^{2+} solutions appeared virtually identical, they have been treated as a single population, and the points in low and normal Ca^{2+} have each been fitted with the Boltzmann equation (eqn (1)) with parameters (g_{max}, V_o and V_e): 2·8 mM-Ca^{2+}, 15·7 nS, −40·8 mV, 3·4 mV; 1 μM-Ca^{2+}, 11·0 nS, −60·3 mV, 2·4 mV. Note that the K^+ conductance can still be activated in 0·1 μM-Ca^{2+}

steps (Fig. 5*A* and *B*). The saturating amplitude is plotted against resonant frequency in Fig. 5*C*, for the fifteen cells in Fig. 4*B* as well as eleven other cells in which no information was available about their Ca^{2+} current. The plot provides strong support for the notion that the K^+ current increases systematically with resonant frequency. Comparison of the tail current kinetics in Fig. 5*A* and *B* indicates that the time constant of decay was about fivefold slower in the cell tuned to the lower frequency, in agreement with earlier observations (Art & Fettiplace, 1987). The time constant for current relaxation at the resting potential has been used previously as an indication of the gating kinetics of the K^+ channels, and has been shown to vary systematically with the resonant frequency of the hair cell.

Variation in the block of the K^+ current by reduced extracellular Ca^{2+}

Since cells which gave a biphasic response in 1 μM Ca^{2+} also often showed a slow component of outward current in normal Ca^{2+} (Fig. 1*B*), one explanation for the results would be that such cells contained two types of K^+ current: a fast Ca^{2+}-activated current and a slower voltage-dependent one. Several observations cast doubt on this conclusion. Firstly, as reported previously (Art & Fettiplace, 1987), all the K^+ current could be completely eliminated by 25 mM TEA. Secondly, the amplitude of the *outward* tail current plotted against membrane potential could be fitted with a single Boltzmann function with no hint of a secondary component. Thirdly, the K^+ current could be blocked if the external Ca^{2+} was reduced to 0·1 μM, as illustrated in Fig. 6*A*. This cell showed a slow augmentation of the outward current in normal Ca^{2+} and a biphasic response in 1 μM Ca^{2+}. However, almost all the residual outward current was blocked in 0·1 μM Ca^{2+}, which implies involvement of a Ca^{2+}-activated K^+ channel. The two components in the onset of the current may therefore reflect either the time course of intracellular Ca^{2+} accumulation or more complex channel kinetics.

Hair cells tuned to very low frequencies (10–20 Hz) retained the majority of their outward current in 1 μM Ca^{2+}, and moreover, the amplitude of this current was unaffected by further reduction of the extracellular Ca^{2+} to 0·1 μM. Figure 6*B* shows activation curves for the outward current in a cell tuned to 10 Hz bathed in normal (2·8 mM), 1 and 0·1 μM Ca^{2+}. Although lowering the Ca^{2+} to 1 μM caused about a 30% reduction in the maximum outward current, no further changes occurred in 0·1 μM Ca^{2+}. The simplest conclusion is that the majority of the K^+ conductance in such cells is voltage activated and not Ca^{2+} activated. This K^+ conductance still possesses steep voltage sensitivity, increasing e-fold in $4{\cdot}6 \pm 1{\cdot}5$ mV (mean $\pm$ S.D., $n = 4$). As with the voltage-dependent Ca^{2+} conductance, the activation curves for the K^+ conductance in low Ca^{2+} were shifted about 20 mV to more negative membrane potentials which may be explained by a surface-charge effect. All cells tuned to very low frequencies also possessed an inward rectifier (see records in Fig. 1*C*) revealed with hyperpolarizing pulses negative to the K^+ equilibrium potential. An inward rectifier was evident in some cells tuned to 50–120 Hz, but not in higher frequency cells.

---

but that its activation curve is shifted 20 mV to more negative membrane potentials. Resonant frequency of hair cell 10 Hz. In all conditions, there was a decline in the maximum current at positive membrane potentials, the reason for which is unknown.

Effects of 10 μM Ca^{2+}

The previous experiments have demonstrated that hair cells with resonant frequencies below 120 Hz may be distinguished by the reduced sensitivity of their K^+ conductances to lowering the extracellular Ca^{2+} concentration to 1 μM. Experiments

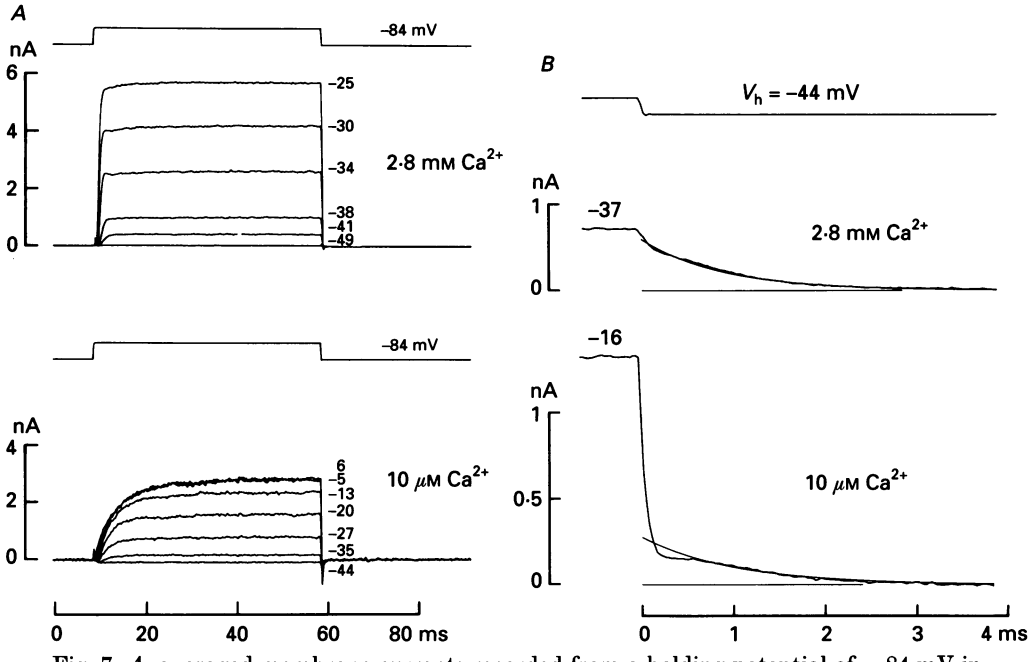

Fig. 7. *A*, averaged membrane currents recorded from a holding potential of −84 mV in 2·8 mM Ca^{2+} (top) and 10 μM Ca^{2+} (bottom), the membrane potential during the step being indicated beside the trace. Note that in low Ca^{2+}, the outward K^+ current can still be activated but its size is reduced and its onset is slowed. *B*, tail currents recorded from the same hair cell at a holding potential of −44 mV. Although the tail currents are smaller and require a larger depolarization for activation, the time constants of the current's decline are similar. The relaxations at the end of the steps have been fitted with single exponentials with time constants of 0·87 ms (2·8 mM Ca^{2+}) and 0·99 ms (10 μM Ca^{2+}). Resonant frequency of hair cell, 240 Hz.

were therefore performed with superfusion with 10 μM Ca^{2+} to test whether cells tuned to higher frequencies showed a uniform sensitivity to Ca^{2+} reduction. For all cells examined, it was possible to activate the majority of the outward current in 10 μM Ca^{2+}, but the onset of the current was generally slowed and strong depolarizations were needed to turn it on (Fig. 7*A*). However, the time constant of relaxation of the current at the end of a depolarizing step was not substantially affected by removal of Ca^{2+}. For the cell illustrated in Fig. 7, which was tuned to 240 Hz, the tail current was smaller in 10 μM Ca^{2+}, but its principal time constant of decay was 0·87 ms in normal Ca^{2+} and 0·99 s in reduced Ca^{2+}. Since this cell had the shortest time constant, it should have been the best candidate for revealing any action of low Ca^{2+} on the relaxation kinetics. Reduction in Ca^{2+} also failed to alter the offset kinetics in another cell tuned to lower frequency with a slower current

relaxation. These observations accord with an earlier finding that the kinetics of the K^+ tail currents were not substantially affected by blocking the Ca^{2+} current with Cd^{2+} (Art & Fettiplace, 1987). This supports the argument that the time constant for current relaxation at the resting potential reflects the gating kinetics of the K^+ channels and is not limited by the rate of diffusion and removal of Ca^{2+}.

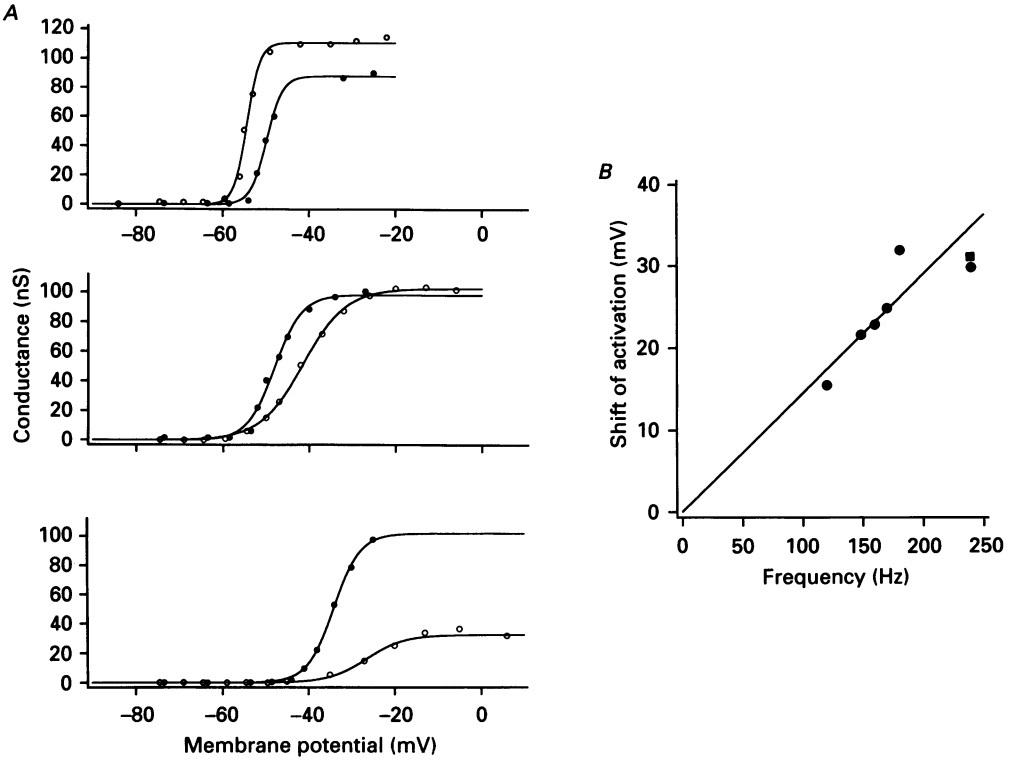

Fig. 8. *A*, activation curves for the K^+ conductance for three hair cells in 2·8 mM Ca^{2+} (●) and 10 μM Ca^{2+} (○). The measurements were derived from voltage clamp records similar to those in Fig. 7, and have been converted to a conductance assuming a reversal potential for the K^+ current of −82 mV. The points are fitted with eqn (1). Resonant frequency (indicated on each graph) and fitting parameters (g_{max} and V_0) in normal and 10 μM Ca^{2+}: respectively 120 Hz, 88 nS, −50 mV, 111 nS, −54 mV; 170 Hz, 97 nS, −48 mV, 100 nS, −41 mV; 240 Hz, 102 nS, −34 mV, 36 nS, −24 mV. *B*, depolarizing shift of half-activation potential in 10 μM Ca^{2+}, corrected for surface-charge effects (see text), is plotted for six different cells against their resonant frequency. The filled square is a second value for the 240 Hz cell, derived from tail current measurements at the resting potential (records in Fig. 7*B*). Straight line through points drawn by eye.

As noted there were marked effects of 10 μM Ca^{2+} on the K^+ conductance, which is plotted against membrane potential for three cells covering an octave in resonant frequency in Fig. 8*A*. These plots were constructed from current–voltage relationships and converted to conductance by assuming a linear single-channel current–voltage curve positive to a reversal potential of −82 mV (Art & Fettiplace, 1987). They have been fitted with the Boltzmann relation (eqn (1)) to determine the

parameters of the conductance. The voltage sensitivity, V_e, had a control value of $2{\cdot}8 \pm 0{\cdot}5$ mV (mean $\pm$ S.D., $n = 6$) which on average was increased to $4{\cdot}3 \pm 1{\cdot}5$ mV ($n = 6$) in 10 μM Ca^{2+}. The steep voltage sensitivity of the control is similar to that reported previously (Art & Fettiplace, 1987), where it was noted that the ratio of voltage sensitivities of the Ca^{2+} channel and the Ca^{2+}-activated K^+ channel was approximately 3, which may indicate the requirement for at least three Ca^{2+} ions to activate the K^+ channels. The *intrinsic* voltage sensitivity of the Ca^{2+}-activated K^+ channel (an e-fold increase in 10–30 mV at a fixed Ca^{2+} concentration; Latorre, Oberhauser, Labarca & Alvarez, 1989) is by comparison lower than that of the Ca^{2+} channel (about 8 mV). The K^+ conductance retains considerable voltage sensitivity in 10 μM Ca^{2+}, which argues that sufficient Ca^{2+} is continuing to enter and bind to sites on the K^+ channel.

For all but one of the cells, the half-activation of the K^+ conductance (V_0) was shifted to more positive membrane potentials but for the lowest frequency cell the shift was negative. Superficially this suggests that the conductance in this cell can be *better* activated in 10 μM Ca^{2+}, though this neglects the fact that Ca^{2+} will enter at more negative membrane potentials due to a concomitant hyperpolarizing shift in the activation of the Ca^{2+} current as described above. To determine the true shift of membrane potential for half-activation, the differences between the control and test measurements were corrected by adding 20 mV to take account of the effects on the Ca^{2+} current itself. The resulting values ranged from 16 to 33 mV, increasing roughly in proportion to resonant frequency (Fig. 8*B*). The maximum conductance achievable was also systematically reduced with increasing resonant frequency (Fig. 8*A*). Thus at a fixed membrane potential (e.g. -20 mV), the Ca^{2+} entry is less effective the higher the resonant frequency of the cell. One explanation for these results is that the affinity of Ca^{2+} for at least one of its binding sites on the Ca^{2+}-activated K^+ channels changes with resonant frequency.

DISCUSSION

Numbers of Ca^{2+} and K^+ channels

A primary goal of this work was to determine whether there were variations in the voltage-dependent Ca^{2+} current among cells of different resonant frequencies. This current flows through channels with properties akin to the L-type Ca^{2+} channel (Fox, Nowycky & Tsien 1987) in its high conductance to Ba^{2+} and sensitivity to blockade by cadmium or dihydropyridines, though in hair cells it activates at membrane potentials about 40 mV more negative than the L-type Ca^{2+} current in nerve cell bodies. Derivation of the amplitude of the Ca^{2+} current from the non-specific cation current flowing through the Ca^{2+} channels in 1 μM external Ca^{2+} confirmed that its size increased in proportion to resonant frequency and that it was almost an order of magnitude larger in cells tuned to the highest frequency than in cells tuned to the lowest frequency. However, the ratio of the Ca^{2+} to K^+ current was independent of resonant frequency (Fig. 4). To estimate the relative numbers of Ca^{2+} and K^+ channels per hair cell, we need values for the single-channel currents. We shall assume that in those cells tuned above 50 Hz, where the K^+ current was Ca^{2+} activated (see below), the single-K^+-channel conductance was constant at about 100 pS (Art & Fettiplace, 1987), which would yield a single-channel current of about

3 pA with an electromotive driving force of about 30 mV. Since we have no direct estimates of the size of the Ca^{2+} channel, we shall use a single-channel current of 0·8 pA obtained from the value of 1·2 pA derived from noise measurements by Roberts, Jacobs & Hudspeth (1990) and corrected for the lower external Ca^{2+} concentration in turtle normal saline. With these values, the currents in Fig. 4*B* can be converted to channel numbers, giving a ratio of numbers of Ca^{2+} to K^+ channels of 2·4; this value is in close agreement with the ratio of 2·6 inferred for frog saccular hair cells (Roberts *et al.* 1990). Roberts *et al.* (1990) argued on the basis of loose-patch recordings that the Ca^{2+} and K^+ channels were co-localized and restricted to small regions of the hair cell membrane which might correspond with the synaptic release sites. If a similar non-uniform distribution of channels were to exist in turtle hair cells, it might imply that cells tuned to higher frequencies had more afferent synaptic contacts than cells tuned to low frequencies. Some support for this notion comes from the electron-microscopic studies of turtle cochlear hair cells by Sneary (1988), who counted about fifteen afferent synapses on apical (low-frequency) cells compared to about ninety on basal (high-frequency) cells. 'Basal hair cells' here refers only to those that lie on the basilar membrane and excludes the category situated on the limbus in the hook region, whose frequency selectivity and physiological role are unknown. The development task of regulating the density of Ca^{2+} and K^+ channels may therefore reduce to one of determining the number of synaptic release sites.

Differences in K^+ channels

A standard test for the existence of a K^+ current activated by Ca^{2+} influx is its abolition by removal of extracellular Ca^{2+}. According to this test, the K^+ current in hair cells with resonant frequencies above 50 Hz was Ca^{2+} activated since it could be blocked by lowering the external Ca^{2+} to 1 or 0·1 μM, whereas the K^+ current in cells tuned from 10 to 20 Hz was scarcely affected by such a manipulation. A caveat to this conclusion is the observation that removal of Ca^{2+} from the bathing solution can alter the gating properties of purely voltage-dependent K^+ currents (Armstrong & Miller, 1990), though this only occurs in the complete absence of extracellular K^+. The differentiation of K^+ currents found in turtle hair cells therefore resembles that in the chick cochlea (Fuchs & Evans, 1990) where the basal hair cells contain a Ca^{2+}-activated K^+ current, whereas apical cells contain a non-inactivating and voltage-dependent K^+ current which has a different single-channel conductance.

In those cells where the K^+ current was Ca^{2+} activated, the sensitivity to lowering the extracellular Ca^{2+} was graded with resonant frequency. Block of the K^+ current in the cell tuned to the lowest frequency required the Ca^{2+} to be reduced to 0·1 μM (Fig. 6) whereas lowering it to only 10 μM caused substantial block in the highest frequency cell (Fig. 8). It is possible that this gradation stems from the fact that high-frequency hair cells, since they possess larger Ca^{2+} currents, may also have more potent Ca^{2+} buffering and extrusion systems that under these conditions reduce the free Ca^{2+} to a lower concentration at the K^+ channel. A simpler explanation is that the K^+ channels require different Ca^{2+} concentrations to activate them at a given membrane potential. Cells tuned to higher frequencies would therefore have Ca^{2+}-activated K^+ channels with faster kinetics but lower sensitivities to Ca^{2+}. An example of this phenomenon has been described for Ca^{2+}-activated K^+ channels in smooth muscle cells (Bolotina, Gericke & Bregestovski, 1991), where two kinetically

distinct channel types of similar unitary conductance could be distinguished: the faster channels had about a four times shorter mean open time and a fivefold lower Ca^{2+} sensitivity. If the K^+ channels in turtle hair cells were to employ a similar mechanism, their range of Ca^{2+} sensitivities should be comparable to the roughly 30-fold range of time constants (0·7–20 ms) observed in cells tuned to more than 50 Hz (Art & Fettiplace, 1987). The maximal sensitivity of large-conductance, Ca^{2+}-activated K^+ channels to changes in Ca^{2+} concentration has been found to vary widely in different cell types (Latorre *et al.* 1989).

Ca^{2+} influx in low external Ca^{2+} concentration

It is surprising that when the external Ca^{2+} concentration was reduced by more than two orders of magnitude from 2·8 mM to 10 μM the K^+ current could still be activated by depolarization. Moreover, the current retained considerable voltage sensitivity (e-fold in 4·3 mV) which argues that the K^+ channels were still being gated by a rise in intracellular Ca^{2+}. A pertinent question concerns how much the Ca^{2+} entry (and hence the concentration of Ca^{2+} at the mouth of the K^+ channel) is reduced in 10 μM Ca^{2+}. Models for the voltage-dependent Ca^{2+} channel (Almers & McCleskey, 1984; Hess & Tsien, 1984) treat it as a single-file pore containing two Ca^{2+} binding sites and, with 10 μM external Ca^{2+}, one of these sites on average would be occupied by a Ca^{2+} ion. Without detailed knowledge of the energy profile within the pore, the channel conductance cannot be accurately calculated. However, some indication can be obtained from the multi-ion pore models developed by Hille & Schwarz (1978). With an energy profile of comparable form to that employed by Almers & McCleskey and Hess & Tsien, the channel conductance will decrease less than linearly with external concentration, and its decline may be more nearly proportional to the square root of external Ca^{2+} over the relevant concentration range (see Fig. 3*B* of Hille & Schwarz, 1978). This implies that the channel conductance will decrease much less than the 280-fold reduction in external Ca^{2+} concentration and may be lowered not much more than tenfold. For Ca^{2+}-activated K^+ channels in a variety of cell types, to achieve the same probability of opening, a tenfold reduction in Ca^{2+} concentration may be offset by about a 40 mV depolarization (Latorre *et al.* 1989), which is comparable to the shifts in voltage sensitivity shown in Fig. 8.

Ca^{2+} extrusion

It is worth emphasizing that the Ca^{2+} fluxes in turtle hair cells are substantial considering the small size of the cell. For a cell subjected to a small depolarization to −40 mV (as could occur *in vivo* due to the continual fluctuations in membrane potential; Crawford & Fettiplace, 1980), the Ca^{2+} current might be of the order of 0·1 nA, corresponding to the entry of 3×10^8 ion s^{-1}. In order to handle this load, the cell must possess an extrusion mechanism of comparable potency. For a Ca^{2+}-ATPase, the maximum substrate turnover is about 200 ions s^{-1} $site^{-1}$ (Hille, 1992, p. 312) and for a carrier, such as the Na^+–Ca^{2+} exchanger, the rate could be ten times larger (Hodgkin, McNaughton & Nunn, 1987). Therefore to keep pace with the Ca^{2+} load would require, depending on the mechanism, between $0{\cdot}15 \times 10^6$ and $1{\cdot}5 \times 10^6$ pump sites per cell (see also Roberts, Jacobs & Hudspeth, 1991). If the pumps were

uniformly distributed over the basolateral surface membrane of area about 750 μm^2, they would have a density of 200–2000 μm^{-2}. However, if the pumps were localized to the potential sites of Ca^{2+} entry at the synaptic zones, their density would need to be up to 100 times larger, which would imply a crystalline array of membrane protein. Clearly an alternative extrusion process, such as concentration of the Ca^{2+} in an intracellular organelle for subsequent export, may need to be postulated. If the organelle were the synaptic vesicle, the Ca^{2+} homeostasis would be effectively self-regulating and could take account of differences between hair cells of different resonant frequencies. However, there is as yet no evidence for Ca^{2+} uptake into synaptic vesicles.

This work was supported by National Institutes of Health grants DC01362 (R. F.) and DC00454 (J. J. A.). J. J. A. was also supported by a Sloan Fellowship and a grant from the Brain Research Foundation of Chicago. We thank Dean Smith for loan equipment and Aaron Fox, Yan-Yi Peng and Larry Trussell for commenting on the manuscript.

REFERENCES

ALMERS, W. & MCCLESKEY, E. W. (1984). Non-selective conductance in calcium channels of frog muscle: calcium selectivity in a single-file pore. *Journal of Physiology* **353**, 585–608.

ALMERS, W., MCCLESKEY, E. W. & PALADE, P. T. (1984). A non-selective cation conductance in frog muscle membrane blocked by micromolar external calcium ions. *Journal of Physiology* **353**, 565–585.

ARMSTRONG, C. M. & MILLER, C. (1990). Do voltage-dependent K^+ channels require Ca^{2+}? A critical test employing a heterologous expression system. *Proceedings of the National Academy of Sciences of the USA* **87**, 7579–7582.

ART, J. J. & FETTIPLACE, R. (1987). Variation of membrane properties in hair cells isolated from the turtle cochlea. *Journal of Physiology* **385**, 207–242.

BOLOTINA, V., GERICKE M. & BREGESTOVSKI, P. (1991). Kinetic differences between Ca^{2+}-dependent K^+ channels in smooth muscle cells isolated from normal and atherosclerotic human aorta. *Proceedings of the Royal Society* B**244**, 51–55.

CRAWFORD, A. C., EVANS, M. G. & FETTIPLACE, R. (1991). The actions of calcium on the mechanoelectrical transducer current of turtle hair cells. *Journal of Physiology* **434**, 369–398.

CRAWFORD, A. C. & FETTIPLACE, R. (1980). The frequency selectivity of auditory nerve fibres and hair cells in the cochlea of the turtle. *Journal of Physiology* **306**, 79–125.

CRAWFORD, A. C. & FETTIPLACE, R. (1981). An electrical tuning mechanism in turtle cochlear hair cells. *Journal of Physiology* **312**, 377–412.

FABIATO, A. & FABIATO, F. (1979). Calculator programs for computing the composition of the solutions containing multiple metals and ligands used for experiments in skinned muscle cells. *Journal de Physiologie* **75**, 463–505.

FETTIPLACE, R. (1987). Electrical tuning of hair cells in the inner ear. *Trends in Neurosciences* **10**, 421–425.

FOX, A. P., NOWYCKY, M. C. & TSIEN, R. W. (1987). Kinetic and pharmacological properties distinguishing three types of calcium currents in chick sensory neurones. *Journal of Physiology* **394**, 149–172.

FRANKENHAEUSER, B. & HODGKIN, A. L. (1957). The action of calcium on the electrical properties of squid axons. *Journal of Physiology* **137**, 218–244.

FUCHS, P. A. & EVANS, M. G. (1990). Potassium currents in hair cells isolated from the cochlea of the chick. *Journal of Physiology* **429**, 529–552.

FUCHS, P. A., EVANS, M. G. & MURROW, B. W. (1990). Calcium currents in hair cells isolated from the cochlea of the chick. *Journal of Physiology* **429**, 553–568.

FUCHS, P. A., NAGAI, T. & EVANS, M. G. (1988). Electrical tuning in hair cells isolated from the chick cochlea. *Journal of Neuroscience* **8**, 2460–2467.

HESS, P. & TSIEN, R. W. (1984). Mechanism of permeation through calcium channels. *Nature* **309**, 453–456.

HILLE, B. (1992). *Ionic Channels of Excitable Membranes*. Sinauer, Sunderland, MA, USA.

HILLE, B. & SCHWARZ, W. (1978). Potassium channels as multi-ion single-file pores. *Journal of General Physiology* **72**, 409–442.

HODGKIN, A. L., MCNAUGHTON, P. A. & NUNN, B. J. (1987). Measurement of sodium–calcium exchange in salamander rods. *Journal of Physiology* **391**, 347–370.

HUDSPETH, A. J. & LEWIS, R. S. (1988). Kinetic analysis of voltage- and ion-dependent conductances in saccular hair cells of the bullfrog, *Rana catesbeiana*. *Journal of Physiology* **400**, 237–274.

KRISHTAL, O. A. & PIDOPLICHKO, V. I. (1980). A receptor for protons in the nerve cell membrane. *Neuroscience* **5**, 2325–2327.

LATORRE, R., OBERHAUSER, A., LABARCA, P. & ALVAREZ, O. (1989). Varieties of calcium-activated potassium channels. *Annual Reviews of Physiology* **51**, 385–399.

LEWIS, R. S. & HUDSPETH, A. J. (1983). Voltage- and ion-dependent conductances in solitary vertebrate hair cells. *Nature* **304**, 538–541.

LUX, H. D., CARBONE, E. & ZUCKER, H. (1989). Block of Na^+ ion permeation and selectivity of Ca^{2+} channels. *Annals of the New York Academy of Sciences* **560**, 94–102.

NERBONNE, J. M. & GURNEY, A. M. (1987). Blockade of Ca^{2+} and K^+ currents in bag cell neurons of *Aplysia californica* by dihydropyridine Ca^{2+} antagonists. *Journal of Neuroscience* **7**, 882–893.

ROBERTS, W. M., JACOBS, R. A. & HUDSPETH, A. J. (1990). Colocalization of ion channels involved in frequency selectivity and synaptic transmission at presynaptic active zones of hair cells. *Journal of Neuroscience* **10**, 3664–3684.

ROBERTS, W. M., JACOBS, R. A. & HUDSPETH, A. J. (1991). The hair cell as a presynaptic terminal. *Annals of the New York Academy of Sciences* **635**, 221–233.

SCHOENMAKERS, T. J. M., VISSER, G. J., FLIK, G. & THEUVENET, P. R. (1992). Chelator: An improved method for computing metal ion concentrations in physiological solutions. *Biotechniques* **12**, 870–879.

SNEARY, M. G. (1988). Auditory receptor of the red-eared turtle. II. Afferent and efferent synapses and innervation patterns. *Journal of Comparative Neurology* **276**, 588–606.

TSIEN, R. Y. & RINK, T. J. (1981). Ca^{2+}-sensitive electrodes: a novel PVC-gelled neutral carrier mixture compared with other currently available sensors. *Journal of Neuroscience Methods* **4**, 73–86.

YELLEN, G. (1982). Single Ca^{2+}-activated non-selective cation channels in neuroblastoma. *Nature* **296**, 357–359.